

Flux-Limited Schemes for the Compressible Navier–Stokes Equations

S. Tatsumi,* L. Martinelli,† and A. Jameson‡
Princeton University, Princeton, New Jersey 08544

Several high-resolution schemes are formulated with the goal of improving the accuracy of solutions to the full compressible Navier–Stokes equations. Calculations of laminar boundary layers at subsonic, transonic, and supersonic speeds are carried out to validate the proposed schemes. It is concluded that these schemes, which were originally tailored for nonoscillatory shock capturing, yield accurate solutions for viscous flows. The results of this study suggest that the formulation of the limiting process is more important than the choice of a particular flux splitting technique in determining the accuracy of computed viscous flows. Symmetric limited positive and upstream limited positive schemes hold the promise of improving the accuracy of the results, especially on coarser grids.

I. Introduction

THE calculation of compressible flows at transonic, supersonic, and hypersonic Mach numbers requires the implementation of nonoscillatory discrete schemes which combine high accuracy with high resolution of shock waves and contact discontinuities. These schemes must also be formulated in such a way that they facilitate the treatment of complex geometric shapes. In the past decade numerous schemes have been developed to meet these requirements in conjunction with the solution of the Euler equations.¹ More recently, the application of such schemes to the Navier–Stokes equations has produced algorithms which have progressively gained acceptance as analysis tools in the aerospace industry. There remains, however, a need to understand and improve Navier–Stokes schemes beyond the current state of the art. The most compelling reason for this rests on the fact that shock capturing requires the construction of schemes which are numerically dissipative, a requirement which could affect the global accuracy of the solution of the physical viscous problem.

In a recent paper² Jameson has shown that a theory of nonoscillatory schemes can be developed for scalar conservation laws based upon the local extremum diminishing (LED) principle that maxima should not increase and minima should not decrease. Moreover, although it is equivalent to the total variation diminishing principle (TVD) for one-dimensional problems, the LED principle can be applied naturally to multidimensional problems on both structured and unstructured meshes. This recent development has shed new light on the principles underlying the construction of both high-resolution switched and flux-limited dissipation schemes. In particular, it allowed the new formulation of two families of flux-limited schemes denominated, symmetric limited positive (SLIP) and upstream limited positive (USLIP), respectively. The present work merges several dissipation schemes based on both the SLIP and USLIP construction with a well-developed cell-centered, finite-volume formulation for solving the two-dimensional Navier–Stokes equations.³ The aim is to analyze and validate these new discretizations for the solution of viscous flow problems.

In Sec. II the design principles of nonoscillatory discrete approximations to a scalar convection equation are reviewed together

with the three alternative flux splitting techniques which have been used to extend the construction to a system of conservation laws. Section III discusses some of the issues arising in the actual implementation of the proposed schemes. It also reviews the multigrid time-stepping algorithm used to compute steady-state solutions. In Sec. IV the results of computations for a laminar boundary layer at subsonic, transonic, and supersonic speeds are compared with theoretical solutions.

II. Design Principles of Nonoscillatory Schemes

Consider the one-dimensional scalar conservation law

$$\frac{\partial v}{\partial t} + \frac{\partial}{\partial x} f(v) = 0 \quad (1)$$

which may be approximated at the grid node j in conservation form by the semidiscrete scheme

$$\Delta x \frac{dv_j}{dt} + (h_{j+\frac{1}{2}} - h_{j-\frac{1}{2}}) = 0 \quad (2)$$

Here $h_{j+\frac{1}{2}}$ is the numerical flux between cell j and $j+1$, and Δx is the mesh interval. It is well known that the least diffusive first-order scheme which satisfies the LED property is the one obtained by approximating the flux as

$$h_{j+\frac{1}{2}} = \frac{1}{2}(f_{j+1} + f_j) - d_{j+\frac{1}{2}}$$

where $d_{j+\frac{1}{2}} = \frac{1}{2}|a_{j+\frac{1}{2}}|\Delta v_{j+\frac{1}{2}} = \alpha_{j+\frac{1}{2}}(v_{j+1} - v_j)$ is a first-order diffusive flux, computed at the cell interface $j + \frac{1}{2}$, as the first difference of v scaled by the absolute value of the approximation of the wave speed $a(v) = \partial f / \partial v$. This is exactly equivalent to a first-order upwind scheme.

Higher order nonoscillatory schemes can be generally derived by introducing antidiffusive terms in a controlled manner, for example, by an appropriate switch or by making use of flux limiters.⁴ Both techniques are reviewed in the following paragraphs.

High-Resolution Switched Schemes

High-resolution switched schemes require the introduction of antidiffusive terms. By subtracting neighboring differences one may produce a third-order diffusive flux

$$d_{j+\frac{1}{2}} = \alpha_{j+\frac{1}{2}} \left\{ \Delta v_{j+\frac{1}{2}} - \frac{1}{2}(\Delta v_{j+\frac{3}{2}} + \Delta v_{j-\frac{1}{2}}) \right\} \quad (3)$$

This scheme generates substantial oscillations in the vicinity of shock waves which can be eliminated by switching locally to the first-order scheme. The switch introduced by Jameson et al.⁴ has proved effective for this purpose and has recently been improved by

Presented as Paper 94-0647 at the AIAA 32nd Aerospace Sciences Meeting, Reno, NV, Jan. 10–13, 1994; received Feb. 1, 1994; revision received June 7, 1994; accepted for publication June 13, 1994. Copyright © 1994 by the American Institute of Aeronautics and Astronautics, Inc. All rights reserved.

*Visiting Research Staff, Department of Mechanical and Aerospace Engineering, Member AIAA.

†Assistant Professor, Department of Mechanical and Aerospace Engineering, Member AIAA.

‡Professor, Department of Mechanical and Aerospace Engineering, Fellow AIAA.

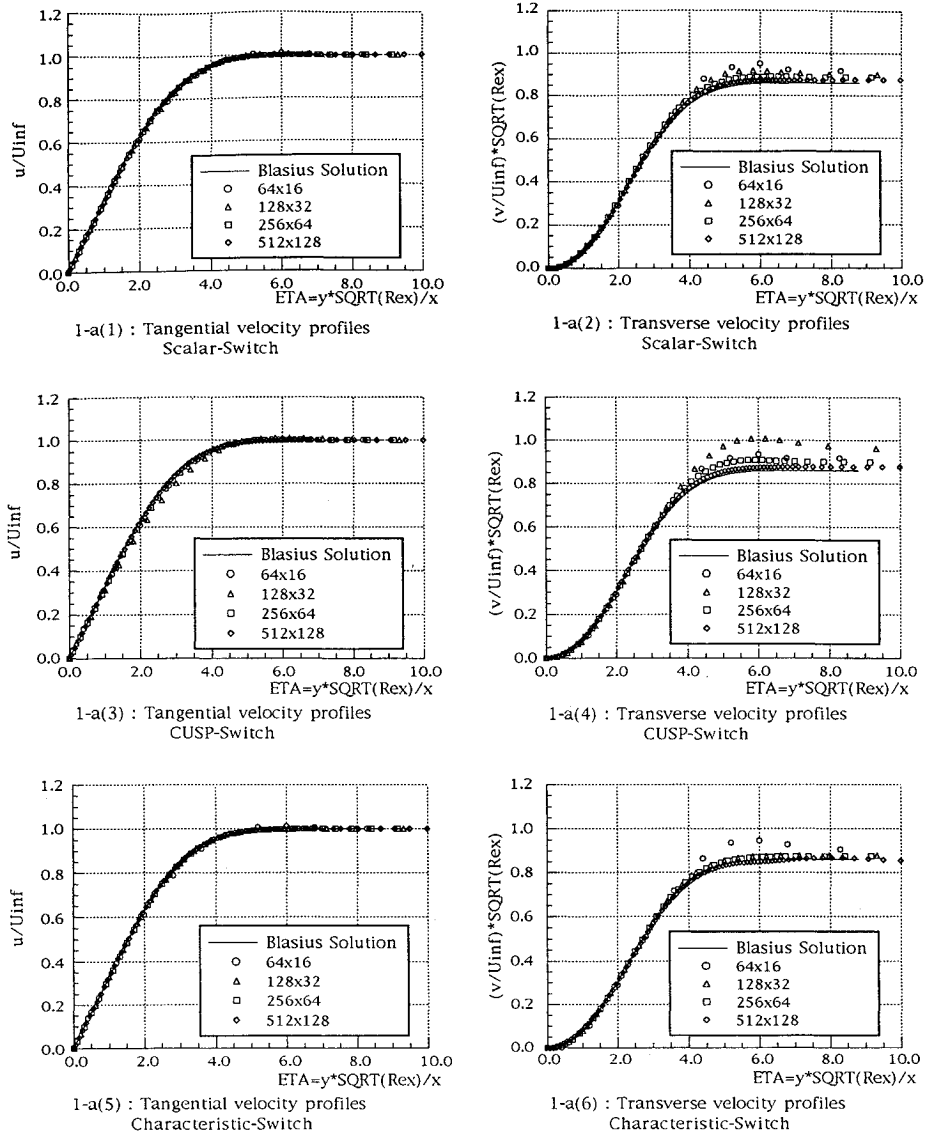


Fig. 1a Grid refinement study on boundary-layer velocity profiles: Mach = 0.15, Re = 1 × 10⁵, and x/L = 0.8; switched schemes.

Table 1 Matrix of the schemes considered

	Scalar splitting	Characteristic splitting	CUSP
Switched	×	×	×
SLIP	×	×	×
USLIP	×	×	×

Swanson and Turkel.⁵ The improved switch is taken as the maximum, in some neighborhood of j , of

$$Q_j = \left| \frac{\Delta v_{j+\frac{1}{2}} - \Delta v_{j-\frac{1}{2}}}{P_0 + (1 - \epsilon)P_1 + \epsilon P_2} \right| \quad (4)$$

where

$$P_1 = |\Delta v_{j+\frac{1}{2}}| + |\Delta v_{j-\frac{1}{2}}|$$

$$P_2 = |v_{j+1}| + 2|v_j| + |v_{j-1}|$$

The value of ϵ is typically 1/2, and P_0 is a threshold to make sure that the denominator cannot be zero. The diffusive flux is now calculated as

$$d_{j+\frac{1}{2}} = \epsilon_{j+\frac{1}{2}}^{(2)} \Delta v_{j+\frac{1}{2}} - \epsilon_{j+\frac{1}{2}}^{(4)} (\Delta v_{j+\frac{3}{2}} - 2\Delta v_{j+\frac{1}{2}} + \Delta v_{j-\frac{1}{2}})$$

where if S is the maximum of Q in the chosen neighborhood, then

$$\epsilon_{j+\frac{1}{2}}^{(2)} = \min(\alpha_1, \alpha_2 S) |a_{j+\frac{1}{2}}|$$

$$\epsilon_{j+\frac{1}{2}}^{(4)} = \max(0, \beta_1 |a_{j+\frac{1}{2}}| - \beta_2 \epsilon_{j+\frac{1}{2}}^{(2)})$$

Usually $\alpha_1 = 1/2$, $\beta_1 = 1/4$ to scale the diffusion to the level corresponding to upwinding, whereas α_2 and β_2 must be chosen to switch the diffusion from third order to first order fast enough near a shock wave.

Symmetric Limited Positive Scheme

Flux limiters offer an alternative avenue for devising high resolution nonoscillatory schemes, and their use dates back to the work of Boris and Book.⁶ A particularly simple way to introduce limiters, proposed by Jameson⁷ in 1984, is to use flux limited dissipation. In this scheme, the third-order diffusion defined by Eq. (3) is modified by the insertion of limiters which produce an equivalent three-point scheme with positive coefficients. Jameson has recently reformulated this scheme as follows.^{2,8}

Let $L(u, v)$ be a limited average of u and v with the following properties:

- P1) $L(u, v) = L(v, u)$.
- P2) $L(\alpha u, \alpha v) = \alpha L(u, v)$.

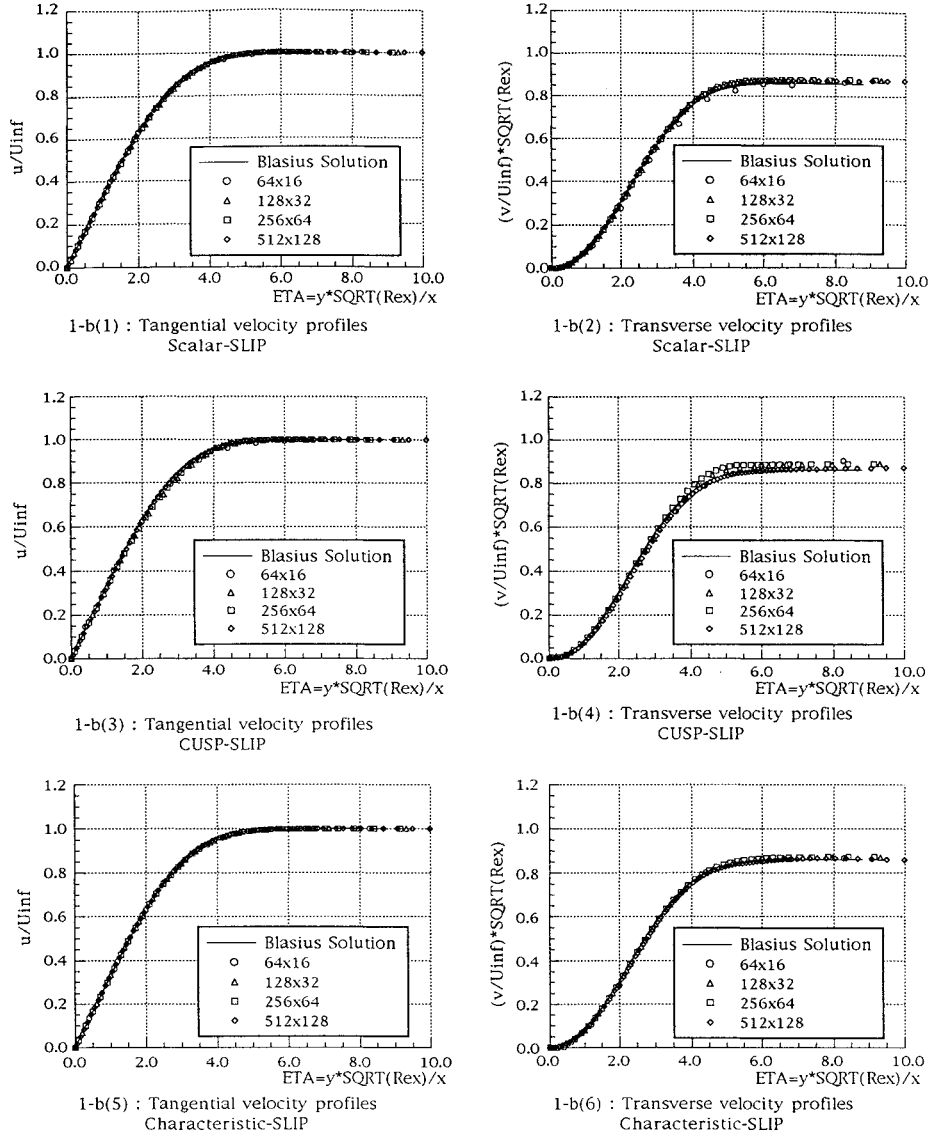


Fig. 1b Grid refinement study on boundary-layer velocity profiles: Mach = 0.15, $Re = 1 \times 10^5$, and $x/L = 0.8$; SLIP schemes.

P3) $L(u, u) = u$.

P4) $L(u, v) = 0$ if u and v have opposite signs.

Note that properties P1-P3 are natural properties of an average, whereas P4 is needed for the construction of an LED scheme.

Then, one defines the diffusive flux for a scalar conservation law as

$$d_{j+\frac{1}{2}} = \alpha_{j+\frac{1}{2}} \left\{ \Delta v_{j+\frac{1}{2}} - L(\Delta v_{j+\frac{3}{2}}, \Delta v_{j-\frac{1}{2}}) \right\} \quad (5)$$

This construction will be referred to as the Symmetric Limited Positive (SLIP) scheme.

The requirement P4 on $L(u, v)$ is the key for constructing a LED scheme. In fact, if $\Delta v_{j+\frac{3}{2}}$ and $\Delta v_{j-\frac{1}{2}}$ have opposite signs, then there is an extremum at either j or $j+1$. In the case of an odd-even mode, however, they have the same sign, which is opposite to that of $\Delta v_{j+\frac{1}{2}}$, so that they reinforce the damping in the same way that a simple central fourth-difference formula would. At the crest of a shock, if the upstream flow is constant, then $\Delta v_{j-\frac{1}{2}} = 0$, and thus $\Delta v_{j+\frac{3}{2}}$ is prevented from canceling any part of $\Delta v_{j+\frac{1}{2}}$ because it is limited by $\Delta v_{j-\frac{1}{2}}$.

Upstream Limited Positive Scheme

By adding the antidiffusive correction purely from the upstream side one may derive a family of Upstream Limited Positive (USLIP)

schemes. Corresponding to the original SLIP scheme defined by Eq. (5), a USLIP scheme is obtained by setting

$$d_{j+\frac{1}{2}} = \alpha_{j+\frac{1}{2}} \left\{ \Delta v_{j+\frac{1}{2}} - L(\Delta v_{j+\frac{1}{2}}, \Delta v_{j-\frac{1}{2}}) \right\} \quad \text{if } a_{j+\frac{1}{2}} > 0$$

$$d_{j+\frac{1}{2}} = \alpha_{j+\frac{1}{2}} \left\{ \Delta v_{j+\frac{1}{2}} - L(\Delta v_{j+\frac{1}{2}}, \Delta v_{j+\frac{3}{2}}) \right\} \quad \text{if } a_{j+\frac{1}{2}} < 0$$

Flux Limiters

A variety of limiters may be defined which meet the requirements (P1-P4). In particular, by defining

$$S(u, v) = 1/2 \{ \text{sign}(u) + \text{sign}(v) \}$$

so that

$$S(u, v) = \begin{cases} 1 & \text{if } u > 0 \text{ and } v > 0 \\ 0 & \text{if } u \text{ and } v \text{ have opposite sign} \\ -1 & \text{if } u < 0 \text{ and } v < 0 \end{cases}$$

one may easily implement any of the three well-known limiters: minmod, Van Leer, or superbee, or construct alternative limiters starting from the more general formulas presented in Ref. 2. In the present study we use a simpler limiter (α mean) which limits the

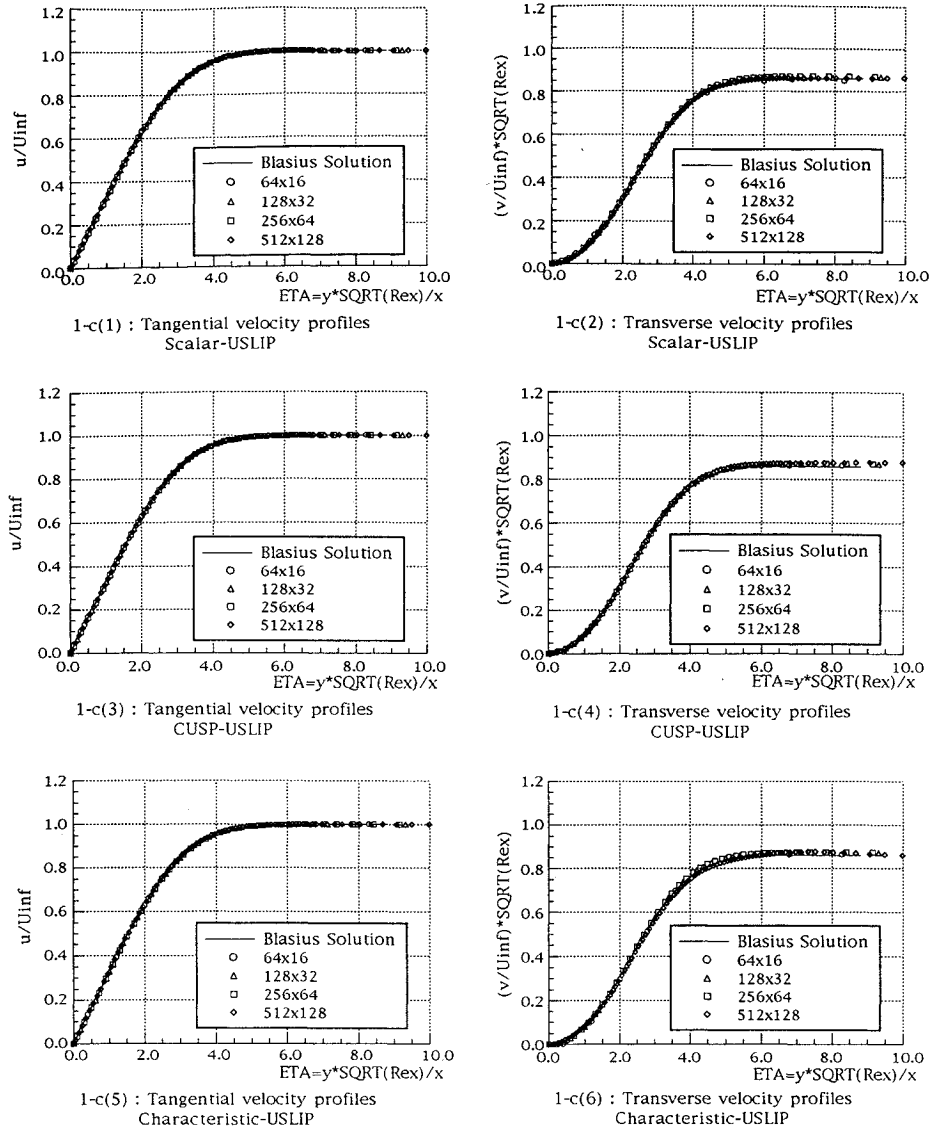


Fig. 1c Grid refinement study on boundary-layer velocity profiles: Mach = 0.15, $Re = 1 \times 10^5$, and $x/L = 0.8$; USLIP schemes.

arithmetic mean by some multiple of the smaller of $|u|$ or $|v|$. It may be cast in the following form:

$$L(u, v) = S(u, v) \min[(|u| + |v|)/2, \alpha|u|, \alpha|v|]$$

In the present study the parameter α was fixed to be equal to 1 with the exception of the calculations with the convective upwind and split pressure (CUSP) splitting where we set $\alpha = 2$.

Extension to Systems of Conservation Laws

The crucial step for extending the construction of nonoscillatory schemes to a system of conservation laws is the generalization of the concept of upwinding and the derivation of stable first-order diffusive schemes. Once this has been achieved, either the high-resolution switched, the SLIP, or the USLIP approach can be used to construct higher order schemes. For the sake of clarity we will consider only the one-dimensional system of equations

$$\frac{\partial \mathbf{w}}{\partial t} + \frac{\partial \mathbf{f}(\mathbf{w})}{\partial x} = 0 \quad (6)$$

For the equations of gas dynamics the solution and flux vectors are

$$\mathbf{w} = \begin{pmatrix} \rho \\ \rho u \\ \rho E \end{pmatrix}, \quad \mathbf{f} = \begin{pmatrix} \rho u \\ \rho u^2 + p \\ \rho u H \end{pmatrix}$$

where ρ is the density, u the velocity, E the total energy, p the

pressure, and H the stagnation enthalpy. If γ is the ratio of specific heats and c the speed of sound, then

$$p = (\gamma - 1)\rho[E - (u^2/2)], \quad c^2 = (\gamma p/\rho)$$

$$H = E + (p/\rho) = (c^2/\gamma - 1) + (u^2/2)$$

In a steady flow H is constant. This remains true for the discrete scheme only if the diffusion is constructed so that it is compatible with this condition.

The three different forms of flux splitting considered in the present study are reviewed next.

Flux Splitting by Characteristic Decomposition

On introduction of Roe's matrix⁹ $A_{j+\frac{1}{2}}$, which is a mean value Jacobian matrix exactly satisfying the condition

$$\mathbf{f}_{j+1} - \mathbf{f}_j = A_{j+\frac{1}{2}}(\mathbf{w}_{j+1} - \mathbf{w}_j)$$

a splitting according to characteristic fields is obtained by decomposing $A_{j+\frac{1}{2}}$ as

$$A_{j+\frac{1}{2}} = T \Lambda T^{-1}$$

where the columns of T are the eigenvectors of $A_{j+\frac{1}{2}}$, and Λ is a diagonal matrix containing the eigenvalues. Hence, the resulting split can be cast as

$$\Delta \mathbf{f}_{j+\frac{1}{2}}^\pm = T \Lambda^\pm T^{-1} \Delta \mathbf{w}_{j+\frac{1}{2}}$$

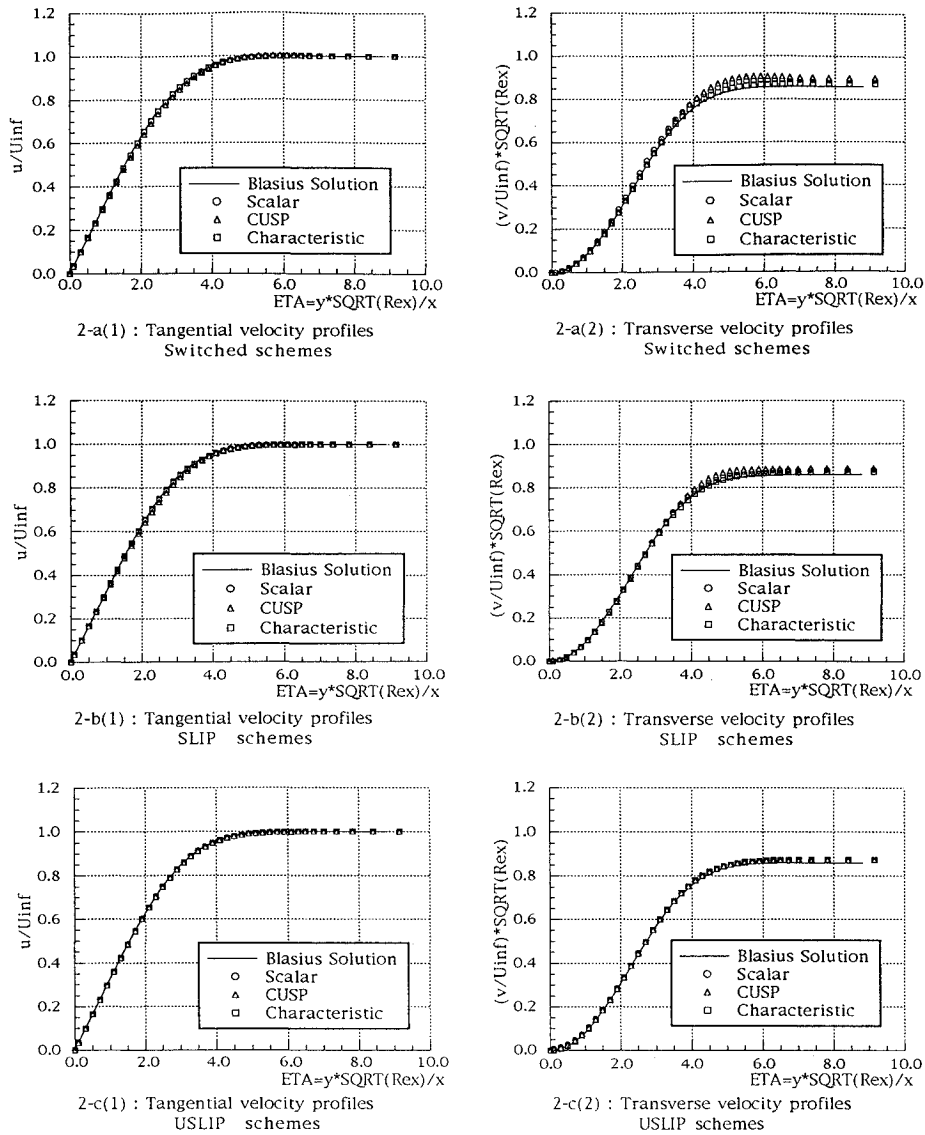


Fig. 2 Boundary-layer velocity profiles: Mach = 0.15, $Re = 1 \times 10^5$, and $x/L = 0.8$.

Now the first-order diffusive flux vector which corresponds to a pure upwind scheme is

$$\mathbf{d}_{j+\frac{1}{2}} = \frac{1}{2}|A_{j+\frac{1}{2}}|(\mathbf{w}_{j+1} - \mathbf{w}_j)$$

where

$$|A_{j+\frac{1}{2}}| = T|\Lambda|T^{-1}$$

and $|\Lambda|$ is the diagonal matrix containing the absolute values of the eigenvalues. This technique will be referred to as characteristic splitting, and it has the advantage that it allows a discrete shock structure with a single interior point. Moreover, it yields more accurate viscous solutions on coarser grids,^{3,10-12} because the eigenvalue q corresponding to the shear and entropy waves approaches zero at the wall.

The implementation of the SLIP construction [Eq. (5)] is now carried out on the differences of the characteristic variables $T^{-1}\Delta\mathbf{w}_{j+\frac{1}{2}}$.

Scalar Splitting

It has been widely demonstrated³⁻⁵ that simple stable schemes can be produced by considering

$$(\mathbf{f}_{j+1} - \mathbf{f}_j)^\pm = \frac{1}{2}(\mathbf{f}_{j+1} - \mathbf{f}_j) \pm \alpha_{j+\frac{1}{2}}(\mathbf{w}_{j+1} - \mathbf{w}_j)$$

This particular splitting gives rise to the scalar diffusive flux

$$\mathbf{d}_{j+\frac{1}{2}} = \alpha_{j+\frac{1}{2}}\Delta\mathbf{w}_{j+\frac{1}{2}}$$

and will be referred to as scalar splitting.

Convective Upwind and Split Pressure Scheme

The eigenvalues of the Jacobian matrix $A = \partial f / \partial \mathbf{w}$ are u , $u + c$, and $u - c$. If $u > 0$ and the flow is locally supersonic ($M = u/c > 1$), all of the eigenvalues are positive, and simple upwinding is thus a natural choice for diffusion in supersonic flow. In general, however, it is convenient to consider the convective and pressure fluxes

$$\mathbf{f}_c = u \begin{pmatrix} \rho \\ \rho u \\ \rho H \end{pmatrix} = u \mathbf{w}_c, \quad \mathbf{f}_p = \begin{pmatrix} 0 \\ p \\ 0 \end{pmatrix}$$

separately. Full upwinding of both f_c and f_p is incompatible with stability in subsonic flow, since pressure waves with the speed $u - c$ would be traveling backward, and the discrete scheme would not have a proper zone of dependence. Since the eigenvalues of $\partial f_c / \partial \mathbf{w}$ are u , u and γu , whereas those of $\partial f_p / \partial \mathbf{w}$ are 0 , 0 , and $-(\gamma - 1)u$, a split with

$$\mathbf{f}^+ = \mathbf{f}_c, \quad \mathbf{f}^- = \mathbf{f}_p$$

leads to a stable scheme¹³ in which downwind differencing is used for the pressure. However, such a scheme does not reflect the true

Table 2 Percentile errors with respect to Blasius solution, station $x/L = 0.8$

Discretization	Cell in boundary layer	% Error in C_f	% Error in δ^*	% Error in θ
Scalar-switched	8	4.05	2.02	1.40
	16	3.05	1.38	0.46
	32	0.89	0.20	0.37
	64	0.51	0.29	0.13
Scalar-SLIP	8	4.88	1.90	1.21
	16	1.87	1.82	0.97
	32	0.26	0.74	0.16
	64	0.09	0.30	0.21
Scalar-USLIP	8	0.21	0.16	3.53
	16	0.75	0.16	1.15
	32	0.61	0.11	0.48
	64	0.34	0.25	0.71
CUSP-switched	8	3.18	3.45	0.10
	16	7.56	7.11	6.16
	32	1.98	1.99	1.32
	64	0.34	0.25	0.24
CUSP-SLIP	8	9.98	3.68	6.44
	16	4.93	2.94	3.32
	32	1.55	1.59	1.09
	64	0.09	0.31	0.18
CUSP-USLIP	8	0.64	1.11	2.58
	16	0.31	0.30	0.98
	32	0.18	0.17	0.43
	64	0.77	0.09	0.60
Characteristic-Switched	8	4.46	2.60	0.66
	16	0.56	0.48	0.68
	32	0.18	0.14	0.50
	64	0.34	0.61	0.89
Characteristic-SLIP	8	1.48	1.02	1.66
	16	1.87	0.26	0.29
	32	1.12	0.09	0.30
	64	0.77	0.59	0.96
Characteristic-USLIP	8	0.21	1.10	2.31
	16	0.31	0.41	0.77
	32	0.18	0.18	0.37
	64	0.34	0.65	0.95

zone of dependence in supersonic flow. Thus, we may seek a scheme which is compatible with stability in subsonic flows and reduces to full upwinding in the supersonic regions.

Full upwinding of the convective flux is achieved by

$$\mathbf{d}_{c_{j+\frac{1}{2}}} = |u_{j+\frac{1}{2}}| \Delta \mathbf{w}_{c_{j+\frac{1}{2}}} = |M| c_{j+\frac{1}{2}} \Delta \mathbf{w}_{c_{j+\frac{1}{2}}}$$

where M is the local Mach number attributed to the interval, whereas full upwinding of the pressure is achieved by

$$\mathbf{d}_{p_{j+\frac{1}{2}}} = \text{sign}(M) \begin{pmatrix} 0 \\ \Delta p_{j+\frac{1}{2}} \\ 0 \end{pmatrix}$$

By introducing blending functions $f_1(M)$ and $f_2(M)$, with the asymptotic behavior $f_1(M) \rightarrow |M|$ and $f_2(M) \rightarrow \text{sign}(M)$ for $|M| > 1$, these equations can be written as

$$\mathbf{d}_{c_{j+\frac{1}{2}}} = f_1(M) c_{j+\frac{1}{2}} \Delta \mathbf{w}_{c_{j+\frac{1}{2}}}$$

$$\mathbf{d}_{p_{j+\frac{1}{2}}} = f_2(M) \begin{pmatrix} 0 \\ \Delta p_{j+\frac{1}{2}} \\ 0 \end{pmatrix}$$

The convective diffusion should remain positive when $M = 0$, whereas the pressure diffusion must be antisymmetric with respect to M . A simple choice is to take $f_1(M) = |M|$ and $f_2(M) = \text{sign}(M)$ for $|M| > 1$, and to introduce blending polynomials in M for $|M| < 1$ which merge smoothly into the supersonic segments. A quartic formula

$$f_1(M) = a_0 + a_2 M^2 + a_4 M^4, \quad |M| < 1$$

preserves continuity of f_1 and df_1/dM at $|M| = 1$ if $a_2 = 3/2 - 2a_0$, $a_4 = a_0 - 1/2$. Then a_0 controls the diffusion at $M = 0$. For transonic flow calculations a good choice is $a_0 = 1/4$, whereas for very high-speed flows it may be increased to $1/2$. Notice that a_0 controls also the amount of dissipation in the inner part of viscous regions. In principle one would prefer to decrease its value as much as possible. In practice, however, it was found that the value of a_0 cannot not be decreased below $1/4$ without impairing convergence. A suitable blending formula for the pressure diffusion is

$$f_2(M) = \frac{1}{2} M(3 - M^2), \quad |M| < 1$$

The diffusion corresponding to the convective terms is identical to the scalar diffusion of Jameson et al.⁴ with a modification of the scaling, whereas the pressure term is the minimum modification needed to produce perfect upwinding in the supersonic zone. The scheme retains the property of the original scheme in that it is compatible with constant stagnation enthalpy in steady flow. If one derives the viscosity corresponding to the flux splitting recently proposed by Liou and Steffen,¹⁴ then it can be shown² that their scheme produces first-order diffusion with a similar general form, and the present scheme may thus be regarded as a construction of artificial viscosity approximately equivalent to Liou-Steffen splitting. The high-resolution scheme is obtained by applying either the limited average or the switch to $(\mathbf{d}_{c_{j+\frac{1}{2}}} + \mathbf{d}_{p_{j+\frac{1}{2}}})$.

III. Implementation

The nine schemes which have been implemented and tested in the present work can be summarized in Table 1. The actual implementation of these schemes to the solution of two-dimensional problems is straightforward: the flux splitting is applied separately in each coordinate direction.

For the scalar dissipation scheme, a blending formula for the spectral radii of the flux Jacobians has been used. Following Ref. 3

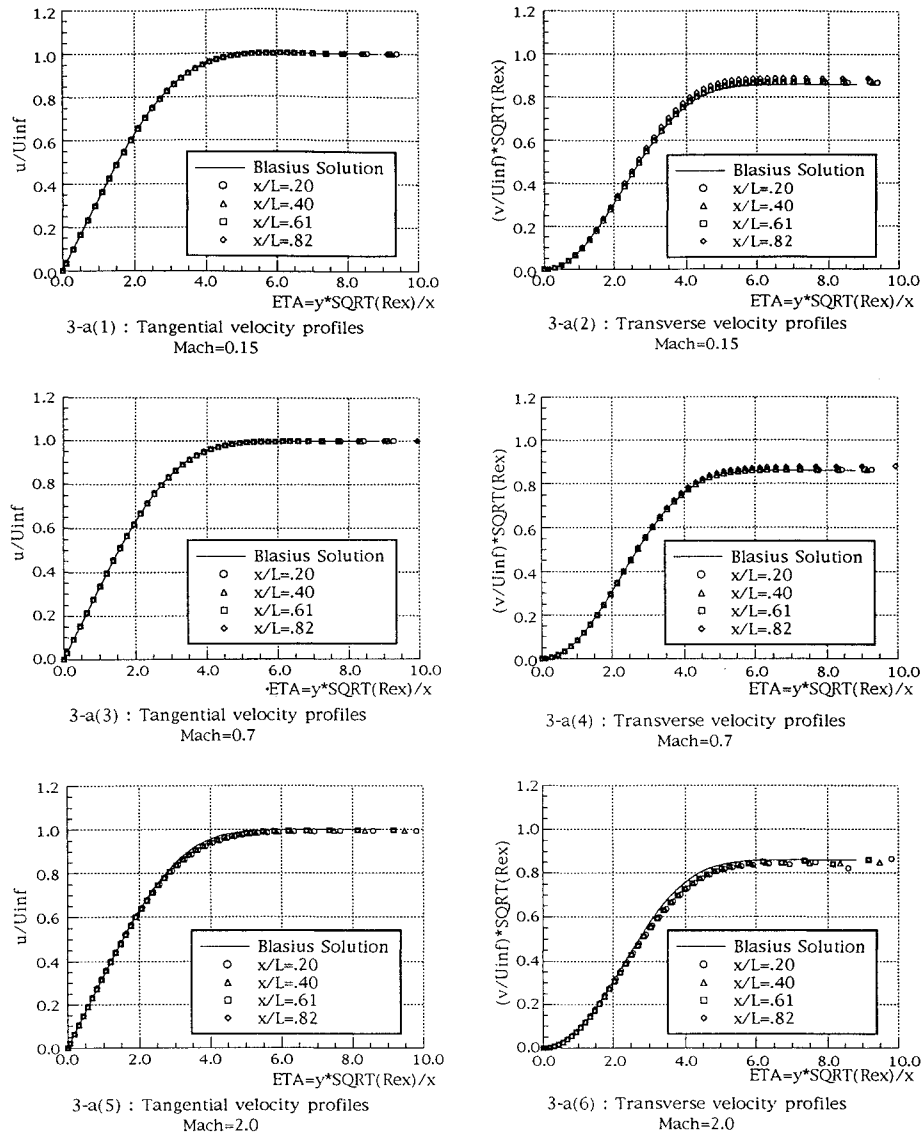


Fig. 3a Boundary-layer velocity profiles: Mach = 0.15, 0.7, and 2.0 (top to bottom), $Re = 1 \times 10^5$, 32 cells in the layer; scalar-switch.

the scaling of the dissipative flux in the I th and J th coordinate directions is taken as follows:

$$\bar{\lambda}_I = \lambda_I \left[1 + \left(\frac{\lambda_J}{\lambda_I} \right)^{\alpha_\epsilon} \right]$$

$$\bar{\lambda}_J = \lambda_J \left[1 + \left(\frac{\lambda_I}{\lambda_J} \right)^{\alpha_\epsilon} \right]$$

Notice that these formulas reduce to a pure directional scaling for $\alpha_\epsilon = 0$, and to a fully isotropic scaling for $\alpha_\epsilon = 1$. This technique has been shown to be effective in reducing the numerical dissipation on highly stretched grids while maintaining good convergence characteristics. For the calculation of the boundary layers presented here, an optimum value of α_ϵ was chosen for each grid density. However, the same value of α_ϵ was maintained on a given grid for all of the Reynolds and Mach numbers. On finer grids, comprising more than 16 cells in the boundary layer, the value $\alpha_\epsilon = 2/3$ was found to give the best results.³ On coarser grids, however, we found that α_ϵ needed to be reduced to $1/4$.

Multigrid Time-Stepping Integration Scheme

Time integration is carried out by making use of a five-stage scheme which requires re-evaluation of the dissipative operators at alternate stages.³ This scheme couples the desirable feature of a wide

stability region along both the imaginary and the real axis with good high-frequency damping. The efficiency of the scheme is enhanced by using implicit residual averaging with variable coefficients and an effective multigrid strategy which utilizes a W cycle.³

In the present study it was found that 100 multigrid cycles are generally sufficient to achieve convergence to a steady state with five orders of magnitude reduction of the rms density residual.

IV. Results

A laminar boundary layer developing over a flat plate at zero incidence provides the test case for the various schemes. A low value of the incoming flow Mach number ($M_\infty = 0.15$), well within the incompressible regime, is selected to make a comparison with a Blasius solution meaningful. Also, this flow condition facilitates the evaluation of the numerical schemes toward their limit of applicability as $M_\infty \rightarrow 0$.

The computational domain is a rectangle with the inflow boundary located two plate lengths upstream of the leading edge and the downstream boundary located at the plate trailing edge. The upper boundary is located at a distance of four plate lengths. The mesh points are clustered in the streamwise direction near the leading edge in order to provide adequate resolution of the flow near the stagnation point. The finest grid contains a total of 512 cells placed in the streamwise direction with 384 of these cells placed along the plate. Within the boundary layer, the grid is equally spaced in the boundary-layer coordinate in the direction perpendicular to the plate. This ensures a constant level of resolution for all of the

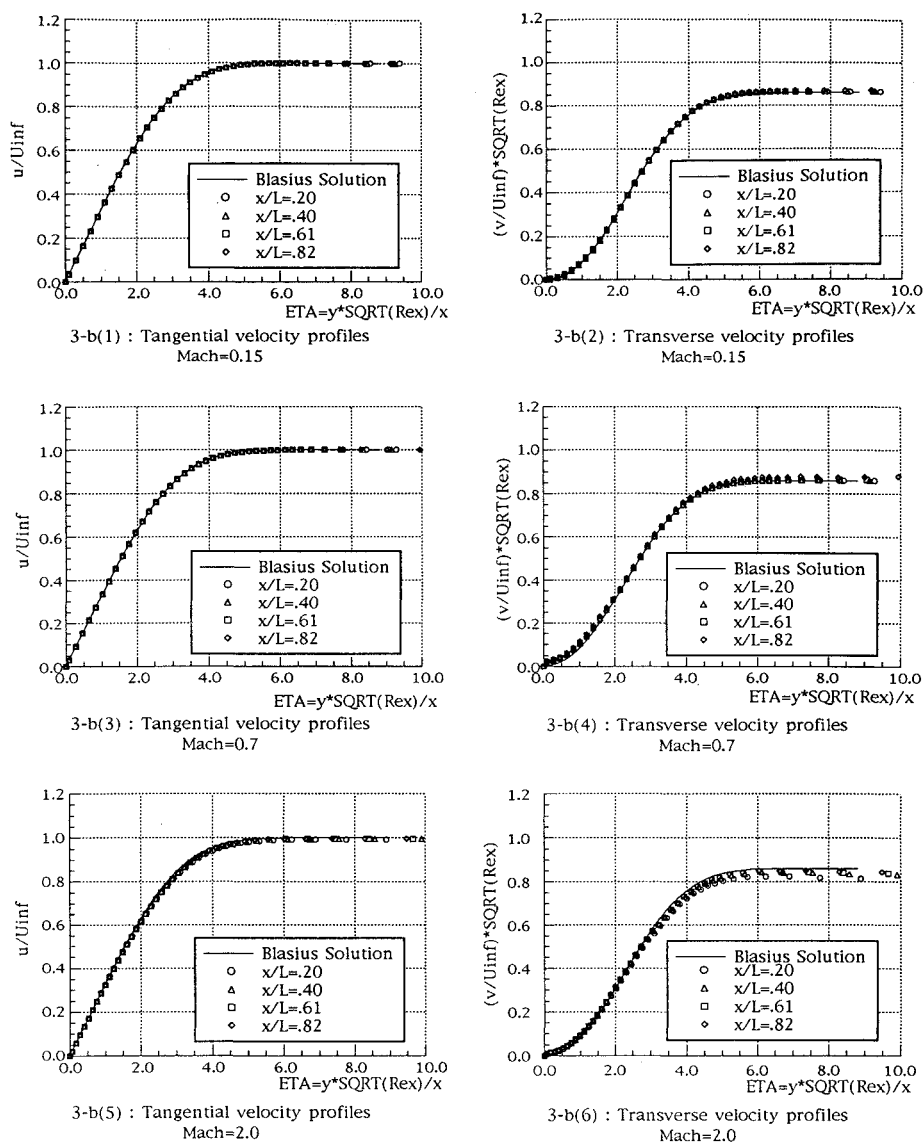


Fig. 3b Boundary-layer velocity profiles: Mach = 0.15, 0.7, and 2.0 (top to bottom), $Re = 1 \times 10^5$, 32 cells in the layer; scalar-USLIP.

boundary-layer profiles. It also ensures an identical resolution in the boundary layer independently of the Reynolds number. Outside of the boundary layer the grid is exponentially stretched toward the far field. The finest grid used contains a total of 128 cells in the direction normal to the plate with half of these cells in the boundary layer. Three coarser grids containing 8, 16, and 32 cells, respectively, within the boundary layer are obtained by elimination of alternate points and are used in the grid refinement study.

No-slip boundary conditions are used on the plate, and symmetry of the incoming flow is assumed upstream of the plate leading edge. Appropriate nonreflective boundary conditions, based on the solution of the one-dimensional Riemann problem normal to the grid lines, are used at the three outer boundaries.

Calculations were performed at Reynolds numbers of 1,000, 10,000, 100,000, and 500,000 based on the length of the plate. However, due to editorial constraints, only the computed results for $Re_\infty = 100,000$ are presented here.

A grid refinement study is presented first, to analyze the accuracy of the nine schemes. The computed results are found to obey the similarity law. Thus, in Fig. 1, we only show the comparison of the computed velocities on four computational grids at one streamwise location ($x/L = 0.8$). Results of the grid refinement study for the three switched schemes are compared in Fig. 1a. It is seen that even the characteristic splitting can produce overshoots in the normal velocity profiles on coarser grids. However, these overshoots are reduced, for all of the three flux splitting techniques considered in this study, if one chooses the SLIP construction. This finding is

documented in Fig. 1b. The USLIP construction seems to give the best results on coarser grids as it is illustrated in Fig. 1c. Notice that all nine schemes produce solutions which converge to the theoretical one as the grid is refined. A more quantitative analysis of the numerical errors is summarized in Table 2 where the percentile errors in skin friction C_f , displacement thickness δ^* , and momentum thickness θ are tabulated. Although the skin friction is obtained directly from the computations, one needs to postprocess the results to obtain an estimate of the integral parameters. In this study we use simple trapezoidal integration applied to the definitions given by Schlichting.¹⁵ We verified that different integration techniques would produce results within 0.5% of those reported in the table.

The results presented in Fig. 2 reinforce the finding of previous studies which have shown that 32 cells are generally sufficient to resolve adequately the viscous layer.³ Moreover, it is seen that the only noticeable differences are in the transverse velocity component and that the results depend more on the construction of the limiting process rather than on the particular form of flux splitting. Notice that the USLIP construction performs slightly better than either the switched or the SLIP formulation, independently of the particular form of flux splitting. This observation provides the motivation for the last set of calculations which are aimed at investigating the behavior of the USLIP schemes over a range of Mach numbers. The results presented in Fig. 3 are obtained for a Reynolds number of 100,000 on a grid with 32 cells in the boundary layer. Figure 3a shows the velocity profiles computed with the standard scalar switched scheme³ for three Mach numbers: $M = 0.15, 0.7,$

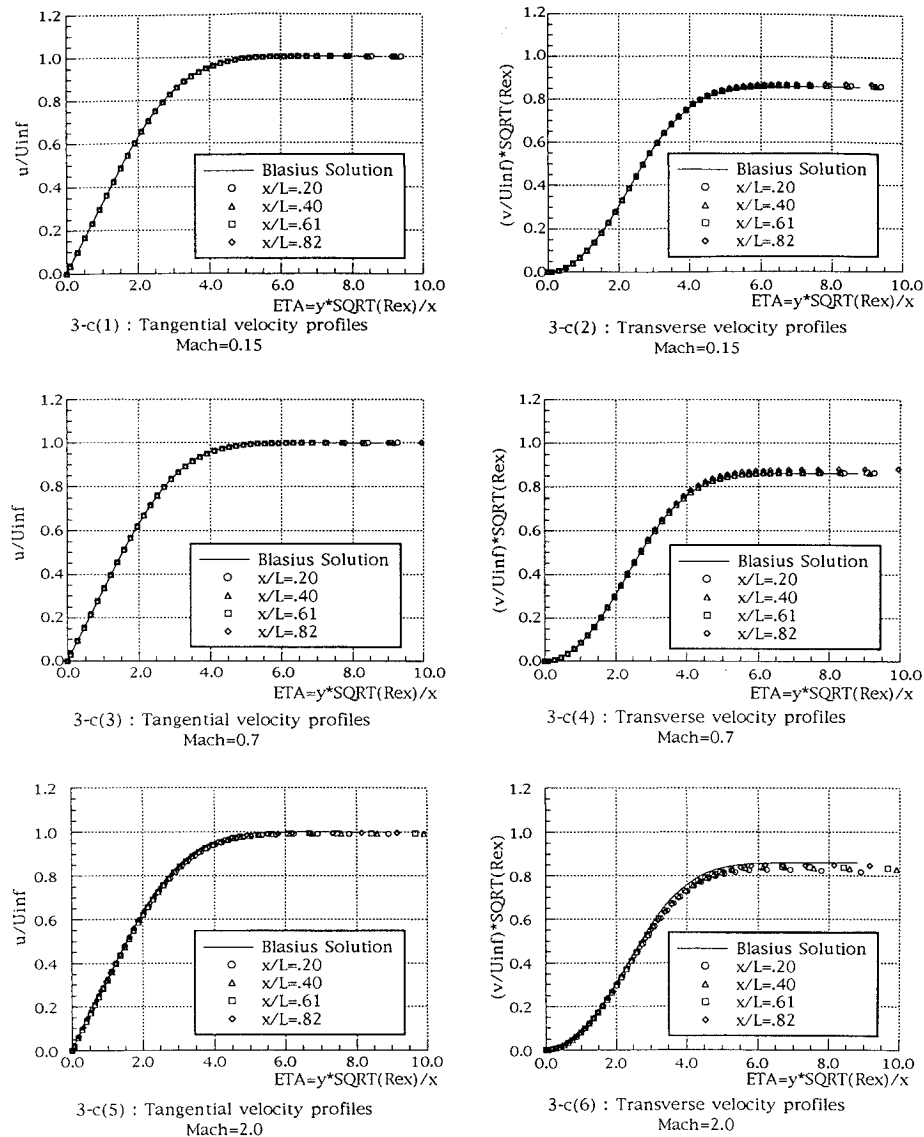


Fig. 3c Boundary-layer velocity profiles: Mach = 0.15, 0.7, and 2.0 (top to bottom), $Re = 1 \times 10^5$, 32 cells in the layer; characteristic-USLIP.

and 2, respectively. The transonic as well as the supersonic results are scaled by using the Illingworth-Stewartson transformation¹⁵ and are again compared with the Blasius solution. The results at four streamwise locations are overplotted to verify the self-similarity of the computed flow. Figures 3b and 3c show similar behavior of the computed results with the scalar-USLIP, and characteristic-USLIP schemes. The results for the subsonic and transonic cases are in excellent agreement with the theory, although some deviations from the theoretical velocity distributions are noticeable for the supersonic one. This discrepancy is partially attributable to the numerical implementation of the Illingworth-Stewartson transformation in the postprocessing stage. In fact, grid refinement studies, not reported here for the sake of brevity, show that the computed solutions presented are indeed grid independent, even for the supersonic case.

V. Concluding Remarks

Several discretization schemes have been developed and applied to the solution of the compressible Navier-Stokes equations. The results presented indicate that these schemes, which have been originally tailored for nonoscillatory shock capturing, yield accurate solutions for viscous flows. In particular, it appears that the construction of SLIP and USLIP schemes holds the promise of improving the accuracy, especially on coarser grids. This result reinforces the observation reported by two of the authors,³ and could have a beneficial impact on three-dimensional applications since current available computers do not allow yet the adequate resolution of complex three-dimensional viscous flows.

The results obtained in the present study with the scalar-switched scheme do not show a degradation in accuracy which is anywhere near as large as that reported by Allmaras.¹ Moreover, our study tends to suggest that the cause for the overshoot observed with the scalar scheme is somewhat different from the one reported in reference,¹⁰ where the poor performance of a scalar scheme for laminar flow at high Reynolds number is attributed to the scaling of the artificial dissipation terms. Our results suggest that the flux-limiting process plays an important role, and that good accuracy can be achieved even with the scalar dissipation in conjunction with the SLIP or the USLIP construction. It appears that the higher order differences required for an antidiffusive construction may result in overshooting unless limiters are introduced.

Preliminary tests on both two-dimensional airfoils¹⁶ and three-dimensional wings, not reported here for the sake of brevity, confirm that the findings of the present study extend to viscous flows with pressure gradients.

Since the SLIP and USLIP constructions can be carried out for unstructured triangular (tetrahedral) meshes, providing multi-dimensional upwinding on arbitrary geometries, it is expected that schemes of this class will also improve the resolution of complex viscous flows on unstructured triangular and tetrahedral grids.

Acknowledgments

The first author gratefully acknowledges Mitsubishi Heavy Industries, Ltd. whose support has made his stay at Princeton University possible. This work has benefited from the generous support of

the Advanced Research Projects Agency under Grant N00014-92-J-1796 and the Air Force Office of Scientific Research under Grant AFOSR-91-0391.

References

- ¹Jameson, A., "Successes and Challenges in Computational Aerodynamics," AIAA Paper 87-1184, June 1987.
- ²Jameson, A., "Computational Algorithms for Aerodynamic Analysis and Design," Technical Rept., INRIA 25th Anniversary Conference on Computer Science and Control, Paris, France, Dec. 1992; *Applied Numerical Methods* (to be published).
- ³Martinelli, L., and Jameson, A., "Validation of a Multigrid Method for the Reynolds Averaged Equations," AIAA Paper 88-0414, Jan. 1988.
- ⁴Jameson, A., Schmidt, W., and Turkel, E., "Numerical Solutions of the Euler Equations by Finite Volume Methods with Runge-Kutta Time Stepping Schemes," AIAA Paper 81-1259, Jan. 1981.
- ⁵Swanson, R. C., and Turkel, E., "On Central-Difference and Upwind Schemes," *Journal of Computational Physics*, Vol. 101, No. 2, 1992, pp. 297-306.
- ⁶Boris, J. P., and Book, D. L., "Flux Corrected Transport, 1 SHASTA, a Fluid Transport Algorithm that Works," *Journal of Computational Physics*, Vol. 11, No. 1, 1973, pp. 38-69.
- ⁷Jameson, A., "A Non-Oscillatory Shock Capturing Scheme Using Flux Limited Dissipation," Mechanical and Aerospace Engineering Rept. 1653, Princeton Univ., Princeton, NJ, April 1984; also, *Lectures in Applied Mathematics*, edited by B. E. Engquist, S. Osher, and R. C. J. Somerville, American Mathematical Society, Pt. 1, Vol. 22, 1984, pp. 345-370.

⁸Jameson, A., "Artificial Diffusion, Upwind Biasing, Limiters and their Effect on Accuracy and Multigrid Convergence in Transonic and Hypersonic Flow," AIAA Paper 93-3359, July 1993.

⁹Roe, P. L., "Approximate Riemann Solvers, Parameter Vectors, and Difference Schemes," *Journal of Computational Physics*, Vol. 43, 1981, pp. 357-372.

¹⁰Allmaras, S., "Contamination of Laminar Boundary Layers by Artificial Dissipation in Navier-Stokes Solutions," *Proceedings of the Conference on Numerical Methods in Fluid Dynamics*, Reading, England, UK, 1992.

¹¹Swanson, R. C., and Turkel, E., "Aspect of a High-Resolution Scheme for the Navier-Stokes Equations," AIAA Paper 93-3372, July 1993.

¹²Garriz, J. A., Vatsa, V. N., and Sanetrik, M. D., "Issues Involved in Coupling Navier-Stokes Mean-Flow and Linear Stability Codes," AIAA Paper 94-0304, Jan. 1994.

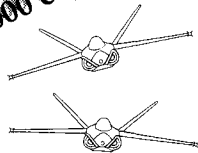
¹³Denton, J. D., "An Improved Time Marching Method for Turbomachinery Flow Calculations," *Journal of Engineering for Gas Turbines and Power*, Transaction of ASME (American Society Mechanical Engineers), Journal of Engineering for Power, Vol. 105, July 1983, pp. 514-524a.

¹⁴Liou, M.-S., and Steffen, C. J., "A New Flux Splitting Scheme," NASA-TM 104404, 1991; also, *Journal of Computational Physics*, Vol. 107, No. 1, July 1993, pp. 23-39.

¹⁵Schlichting, H., *Boundary Layer Theory*, 7th ed., McGraw-Hill, New York, 1979.

¹⁶Tatsumi, S., "Design, Implementation, and Validation of Flux Limited Schemes for the Solution of the Compressible Navier-Stokes Equations," Mechanical and Aerospace Engineering Rept. 2009, Princeton Univ., Princeton, NJ, Aug. 1994.

10,000 copies sold!



"The addition of the computer disk should greatly enhance the value of this text. The text is a one-of-a-kind resource for teaching a modern aircraft design course."
J.F. Marchman,
Virginia Institute of Technology

Aircraft Design: A Conceptual Approach Second Edition

Daniel P. Raymer

Now you get everything that made the first edition a classic and more. *Aircraft Design: A Conceptual Approach* fills the need for a textbook in which both aircraft analysis and design layout are covered equally, and the interactions between these two aspects of design are explored in a manner consistent with industry practice. New to this edition: Production methods, post stall maneuver, VTOL, engine cycle analysis, plus a complete design example created for use with RDS-STUDENT.

1992, 739 pp, illus, Hardback
ISBN 0-930403-51-7
AIAA Member \$53.95, Nonmembers \$66.95
Order #: 51-7(945)

RDS-STUDENT: Software for Aircraft Design, Sizing, and Performance Version 3.0

Daniel P. Raymer

A powerful new learning tool, RDS-STUDENT lets students apply everything they learn—as they learn it. The software package includes comprehensive modules for aerodynamics, weights, propulsion, aircraft data file, sizing and mission analysis, cost analysis, design layout, and performance analysis, including takeoff, landing, rate of climb, P_s/f_s , turn rate and acceleration. RDS-STUDENT also provides graphical output for drag polars, L/D ratio, thrust curves, flight envelope, range parameter, and other data.

1992, 71 pp User's Guide and 3.5" disk
ISBN 1-56347-047-0
AIAA Members \$54.95, Nonmembers \$69.95
Order #: 47-0(945)

Buy Both
and Save!

Aircraft Design, 2nd Edition and RDS-STUDENT
AIAA Members \$95.95, Nonmembers \$125.95
Order #: 51-7/47-0(945)

Place your order today! Call 1-800/682-AIAA



American Institute of Aeronautics and Astronautics

Publications Customer Service, 9 Jay Gould Ct., P.O. Box 753, Waldorf, MD 20604
FAX 301/843-0159 Phone 1-800/682-2422 8 a.m. - 5 p.m. Eastern

Sales Tax: CA residents, 8.25%; DC, 6%. For shipping and handling add \$4.75 for 1-4 books (call for rates for higher quantities). Orders under \$100.00 must be prepaid. Foreign orders must be prepaid and include a \$20.00 postal surcharge. Please allow 4 weeks for delivery. Prices are subject to change without notice. Returns will be accepted within 30 days. Non-U.S. residents are responsible for payment of any taxes required by their government.